PHYSICAL REVIEW A **89**, 021601(R) (2014)

Quenching to unitarity: Quantum dynamics in a three-dimensional Bose gas

A. G. Sykes,[1] J. P. Corson,[1] J. P. D'Incao,[1] A. P. Koller,[1] C. H. Greene,[2] A. M. Rey,[1] K. R. A. Hazzard,[1] and J. L. Bohn[1]
[1]*JILA, University of Colorado and National Institute of Standards and Technology, Boulder, Colorado 80309-0440, USA*
[2]*Department of Physics, Purdue University, West Lafayette, Indiana 47907-2036, USA*
(Received 30 August 2013; revised manuscript received 18 November 2013; published 3 February 2014)

We study the dynamics of a zero-temperature Bose condensate following a sudden quench of the scattering length from noninteracting to unitarity (infinite scattering length). We apply three complementary approaches to understand the momentum distribution and loss rate. First, using a time-dependent variational ansatz for the many-body state, we calculate the dynamics of the momentum distribution. Second, we demonstrate that, at short times and large momenta compared to those set by the density, the physics can be understood within a simple, analytic two-body model. We make a quantitative prediction for the evolution of Tan's contact and find features in the momentum distribution that are absent in equilibrium. Third, we study three-body loss at finite density under the same dynamic scenario. We find lifetimes that are long compared to the saturation times of large-momentum modes, and we relate this result to the three-body inelasticity parameter.

DOI: 10.1103/PhysRevA.89.021601 PACS number(s): 67.85.−d, 03.75.−b, 67.10.Ba

Ultracold atomic physics offers unique opportunities to study strongly correlated systems due to the tunability of the s-wave scattering length a via Fano-Feshbach resonances [1]. Particularly interesting are quantum gases at unitarity, where a is much larger than any other length scale in the system. Here, the physics is highly nonperturbative due to strong correlations. Such systems are predicted to exhibit universal behavior which depends only on the density. Investigations to date have predominantly focused on the Fermi gas, where three-body loss is suppressed by statistical repulsion [2]. Over the last decade, a general consensus has emerged on many issues surrounding the unitary Fermi gas [3–8]. Theoretical understanding of the unitary Bose gas is less developed. Although experiments have been able to measure beyond-mean-field effects, such as the famous Lee-Huang-Yang correction [9,10] for values of $na^3 \lesssim 7 \times 10^{-3}$ (n being the number density), progress towards unitarity with $na^3 \gg 1$ is hampered by the catastrophic scaling of three-body loss. At zero temperature in the dilute gas, where $na^3 \ll 1$ and $a \gg r_{\mathrm{vdW}}$ (the van der Waals length), the three-body recombination constant scales universally as $L_3 \propto \hbar a^4/m$ [11–16]. This a^4 scaling renders any adiabatic transition from the weakly interacting limit to the unitary limit impractical [17,18]. One approach to limit loss involves *nondegenerate* unitary Bose gases [19,20], where low-recombination regimes can exist [21].

A brazen new approach adopted in a recent experiment [22] utilizes an effectively diabatic quench of the scattering length to unitarity, with the initial gas temperature well below degeneracy. Dimensional analysis requires both the loss rate and the equilibration rate to scale as $n^{2/3}$. The experiment observed the equilibration of large-momentum modes over a faster time scale than the decay, indicating a substantial difference between the prefactors of the two rates. This exciting result indicates a unique route to the realization of a metastable unitary Bose gas.

In this Rapid Communication, we examine the short-time dynamics following a quench from noninteracting ($a \approx 0$) to unitarity ($a = \infty$). We focus on the coherent evolution of the momentum distribution (particularly at large momenta) and the time scale for three-body loss. We study and compare results from several distinct models to understand different aspects of the problem. First, we use a time-dependent variational ansatz in a many-body theory with *mean-field-like* approximations [23] and a regularized effective potential, expecting the results to be valid at short times when the condensate depletion is small. We then compare the results of this many-body calculation to an exactly solvable two-body model [24]. We argue that the early stages of time evolution correspond to the buildup of local correlations between nearby particles (see Fig. 1). The *earliest* stages of this evolution would therefore be related to the dynamics of a two-body system; a similar rationale was employed for weaker interactions in Refs. [25,26]. This seemingly naive argument provides intuitive understanding and a simple analytic formula which agrees remarkably well with the many-body model at large momentum and short times. This is perhaps less surprising in light of the connection between Tan's contact (which determines the occupation of large-momentum modes) and two-body collision physics [27–29]. We also discuss the results of a three-body model that is designed to explain three-body loss at finite density. We compare the time scales for which coherent dynamics occurs to the time scale for three-body loss, finding results which are consistent with Ref. [22]. Specifically, we observe that the dynamics of large-momentum modes saturates before any appreciable three-body loss occurs. Finally, we make predictions for future experiments regarding the structure of the momentum distribution and the contact dynamics.

Many-body model. We consider the Hamiltonian

$$\hat{H} = \sum_{\mathbf{k}} \epsilon_{\mathbf{k}} \hat{a}^\dagger_{\mathbf{k}} \hat{a}_{\mathbf{k}} + \frac{1}{2V} \sum_{\mathbf{k}_1,\mathbf{k}_2,\mathbf{q}} \tilde{U}(\mathbf{q}) \hat{a}^\dagger_{\mathbf{k}_1+\mathbf{q}} \hat{a}^\dagger_{\mathbf{k}_2-\mathbf{q}} \hat{a}_{\mathbf{k}_1} \hat{a}_{\mathbf{k}_2}, \quad (1)$$

where V is the system volume, $\tilde{U}(\mathbf{q}) = \int d^3\mathbf{r}\, e^{-i\mathbf{q}\cdot\mathbf{r}} U(\mathbf{r})$ is the Fourier transform of the interaction potential, $\epsilon_{\mathbf{k}} = \hbar^2 k^2/2m$, and $\hat{a}_{\mathbf{k}}$ is a bosonic annihilation operator for a particle of momentum $\hbar\mathbf{k}$. We use a time-dependent generalization of the ansatz used in Refs. [30,31]:

$$|\Psi_{\mathrm{var}}(t)\rangle = \mathcal{A}(t) \exp\left[c_0(t)\hat{a}^\dagger_0 + \sum_{\mathbf{k}\cdot\hat{\mathbf{z}}>0} g_{\mathbf{k}}(t) \hat{a}^\dagger_{\mathbf{k}} \hat{a}^\dagger_{-\mathbf{k}} \right] |0\rangle, \quad (2)$$

where $\mathcal{A}(t)$ is a normalization constant that depends on the variational parameters $\{c_0(t), g_{\mathbf{k}\neq 0}(t)\}$, and $|0\rangle$ is the

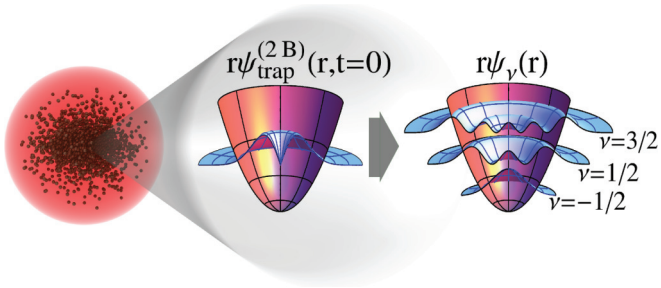

FIG. 1. (Color online) Immediately following a quench in the scattering length, the dynamics originates in *causally isolated* regions of the cloud. The collective effect of other particles in the system is modeled by an artificial trap [25,26], tailored to give the particles a mean interparticle separation which is consistent with that of the many-body system.

particle vacuum. Provided the condensate depletion is small, this ansatz is justified by the Bogoliubov-type idea that the condensed mode behaves as a coherent state and the excited particles are generated in pairs by the dominant term $\hat{a}^\dagger_{\mathbf{k}}\hat{a}^\dagger_{-\mathbf{k}}\hat{a}_0\hat{a}_0$ in $\hat{H}$. Our variational parameters are related to momentum occupations via $n_0(t) = |c_0(t)|^2$ and $n_{\mathbf{k}}(t) = |g_{\mathbf{k}}(t)|^2/(1-|g_{\mathbf{k}}(t)|^2)$. We note that average total particle number and energy are conserved.

In terms of these amplitudes, the equations of motion for the system are $i\hbar\dot{c}_0 = \partial\langle\hat{H}\rangle/\partial c_0^*$ and $i\hbar\dot{g}_{\mathbf{k}} = (1-|g_{\mathbf{k}}|^2)\partial\langle\hat{H}\rangle/\partial g_{\mathbf{k}}^*$ [32]. We solve these coupled equations numerically, where our initial condition is chosen to be a noninteracting gas such that $g_{\mathbf{k}}(0) = 0$ for all $\mathbf{k} \neq 0$. The short-range interactions are modeled with an attractive spherical square well $U(\mathbf{r})mr_0^2/\hbar^2 = -(\frac{\pi}{2})^2\Theta(r_0 - r)$, where r_0 is the range of the potential and is assumed to be much smaller than the interparticle spacing. The depth of the well is chosen such that there is a single two-body bound state at threshold, so the scattering length diverges [33]. We have found that the dynamics for momenta $k \ll 1/r_0$ does not depend on the specific choice of r_0 as long as $nr_0^3 \ll 1$; additionally, the computed dynamics is found to scale universally with the appropriate density units. We discuss the results of this model after introducing a complementary two-body model.

Two-body model. Based on the idea of dynamics originating in causally isolated regions of the gas (see Fig. 1), we consider the dynamics of a two-body wave function in an artificial trap $\psi^{(2B)}_{trap}(\mathbf{r};t) = \sum_\nu c_\nu\psi_\nu(\mathbf{r})e^{-iE_\nu t/\hbar}$, with $\mathbf{r} = \mathbf{r}_1 - \mathbf{r}_2$ being the relative coordinate. The summation is over all eigenvalues or states [24] of the Hamiltonian

$$\left[\frac{-\hbar^2}{2\mu}\nabla^2_{\mathbf{r}} + \frac{1}{2}\mu\omega_{\rm ho}r^2 + \frac{2\pi\hbar^2 a}{\mu}\delta^{(3)}_{\rm reg}(\mathbf{r})\right]\psi_\nu = E_\nu\psi_\nu, \qquad (3)$$

with $\mu = m/2$ being the reduced mass, and $\delta^{(3)}_{\rm reg}(\mathbf{r}) = \delta(\mathbf{r})\partial_r r$ is the Fermi pseudopotential. We expect this approach to be relevant on time scales much less than the trap period. The coefficients $c_\nu = \int d^3\mathbf{r}\ \psi^{(2B)}_{trap}(\mathbf{r};0)\psi^*_\nu(\mathbf{r})$ are determined by the initial condition, which we choose to be the noninteracting ground state $\psi^{(2B)}_{trap}(\mathbf{r};0) = \pi^{-3/4}a_{\rm ho}^{-3/2}e^{-r^2/2a_{\rm ho}^2}$, where $a_{\rm ho} = \sqrt{\hbar/\mu\omega_{\rm ho}}$ is the harmonic oscillator length. This trap length $a_{\rm ho}$ is the only free parameter in the two-body model. We choose $a_{\rm ho}$ such that the average separation of the two particles is $\langle r\rangle = \int d^3\mathbf{r}\, r|\psi^{(2B)}_{trap}(\mathbf{r};0)|^2 = \frac{2a_{\rm ho}}{\sqrt{\pi}} := (4\pi n/3)^{-1/3}$, where n is the initial density of the actual many-body system. Thus, the two particles initially have a mean interparticle separation that is consistent with the many-body system. At unitarity, the eigenvalues of Eq. (3) are $E_\nu = (2\nu + \frac{3}{2})\hbar\omega_{\rm ho}$, with $\nu \in \{-\frac{1}{2}, \frac{1}{2}, \frac{3}{2}, \ldots\}$, and the normalized eigenstates [24] are $\psi_\nu(\mathbf{r}) = A_\nu\frac{1}{\tilde{r}}e^{-\tilde{r}^2/2}\mathrm{H}_{2\nu+1}(\tilde{r})$. Here, H_n is a Hermite polynomial $\tilde{r} = r/a_{\rm ho}$, and $A_\nu = \frac{2^{1-\nu}}{\pi(2\nu)!!a_{\rm ho}^{3/2}}\sqrt{\frac{\Gamma(1+\nu)}{\Gamma(3/2+\nu)}}$. We then find $c_\nu = -\frac{(-2)^{\nu+1/2}\pi^{1/4}(2\nu)!!}{\nu}a_{\rm ho}^{3/2}A_\nu$. With the momentum-space eigenstates $\tilde{\psi}_\nu(\mathbf{k})$ [32], it is straightforward to calculate the momentum distribution $n_k^{(2B)}(t) = (2\pi)^{-3}|\sum_\nu c_\nu\tilde{\psi}_\nu(\mathbf{k})e^{-iE_\nu t/\hbar}|^2$. We assume that the center of mass is untrapped, in which case the total momentum distribution coincides with the relative momentum distribution.

Results. For $ka_{\rm ho} \gg 1$ and $\omega_{\rm ho}t \ll 1$, the momentum distribution dynamics reduces to the analytic formula

$$n_k^{(2B)}(t) = \frac{A}{k^4}\left|\frac{2j}{\sqrt{\pi}}\sqrt{t\mu/\hbar}e^{i\frac{\pi}{2}} - \frac{1}{k}\mathrm{erf}(j\sqrt{\tau})\right|^2, \qquad (4)$$

where $j = e^{-i\pi/4}/\sqrt{2}$ and $\tau = t/\tau_k$ with $\tau_k = \mu/(\hbar k^2)$ denoting a characteristic time scale for each momentum mode. This formula is independent of the trapping potential except through the prefactor A, which we have explicitly verified [32]. We note the presence of a $1/k^5$ term in Eq. (4). None of the equilibrium eigenstates display such behavior. Indeed, any eigenstate can be written $\tilde{\psi}_\nu(k \to \infty) = D_2/k^2 + D_4/k^4$ where D_2 and D_4 depend only on ν. This $1/k^5$ term is an intriguing feature of our nonequilibrium two-body correlations. In equilibrium, corrections to n_k at order $1/k^5$ only arise from three-body contact conditions in the form $n_k = C_2/k^4 + C_3/k^5 \times$(a log-periodic function of k) [34–36]. Our work shows how the momentum distribution can contain additional $1/k^5$ dependence from two-body physics when the system is far from equilibrium.

Figure 2 shows the momentum distribution for two rescaled times $\omega_{\rm F}t$, where $\omega_{\rm F} = k_{\rm F}^2\hbar/2m$ is the Fermi frequency, and

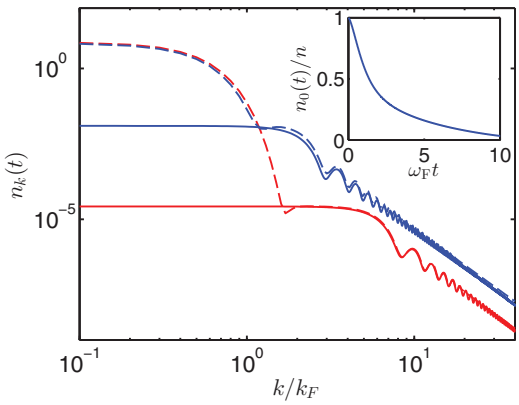

FIG. 2. (Color online) The momentum distribution for two different times $\omega_{\rm F}t = 0.05$ (shown in red) and $\omega_{\rm F}t = 0.4$ (shown in blue). The solid lines show results from the many-body model, and the dashed lines show results from the harmonically trapped two-body model. Note that $n_k = n(2\pi)^3 n_k^{(2B)}$ [32]. The inset shows dynamics of the condensate fraction within the many-body model.

$k_F = (6\pi^2 n)^{1/3}$ is the Fermi momentum [37]. The agreement between two- and many-body models at high momenta $k_F \ll k \ll 1/r_0$, and short times $\omega_F t \ll 1$, is excellent. One can understand the qualitative agreement by recognizing that the large-momentum behavior of n_k in a many-body system is determined by the short-distance behavior of the pair correlation function, which in turn is determined by the solution of an appropriate two-body Schrödinger equation. The excellent quantitative agreement depends strongly on fixing the free parameter in the two-body model (a_{ho}) such that $\langle r \rangle = (4\pi n/3)^{-1/3}$. Fixing to this value agrees intuitively with what one might expect based on the mean interparticle spacing in the many-body system. At high momenta, both calculations reveal a dependence $n_k \sim 1/k^4$ (the oscillations are of order k^{-5}). This behavior is characteristic of short-range two-body interactions and leads to the thermodynamic parameter known as the contact $C \equiv \lim_{k\to\infty} k^4 n_k$ (normalized such that $\sum_{\mathbf{k}} n_{\mathbf{k}} = N$) [27]. Our time-dependent simulations show that the $1/k^4$ tail first appears at large momenta and propagates into smaller momenta. The contact initially exhibits linear growth, which can be extracted from the asymptotics of the two-body model [32]

$$C(t) = 2048\left(\frac{2n^4}{3^5\pi^7}\right)^{1/3}\omega_F t. \tag{5}$$

This formula agrees (within 6%) with a linear fit to the many-body numerical data which predicts $C(t) \approx 26.9(1) n^{4/3}\omega_F t$ for $\omega_F t \lesssim 0.2$.

The oscillations observed in both Figs. 2 and 3(b) are a general feature of the coherent dynamics following a quench in the scattering length (also observed in the weakly interacting regime [38–40]). The many-body and two-body models agree very well on the amplitude, frequency, and phase of these oscillations. Although these oscillations were not discussed in Ref. [22], their observation may be possible with only a modest increase in signal to noise.

As time exceeds $\omega_F t \gtrsim 1$, the two-body model is heavily influenced by the artificial trap and becomes invalid. However, as seen in Fig. 3(a), the many-body model predicts a relaxation of the contact into an asymptotic value of $C \approx 12 n^{4/3}$. Predictions for C in the unitary ground state can be found in Refs. [41–43] and vary from $C \approx 10$–$32 n^{4/3}$. From Fig. 3(a), we observe the contact reaches an equilibrated value beyond $\omega_F t \approx 1$. We note that our predictions at large times are not rigorously justified because the condensate depletion (see inset in Fig. 2) is large enough to violate assumptions of the ansatz

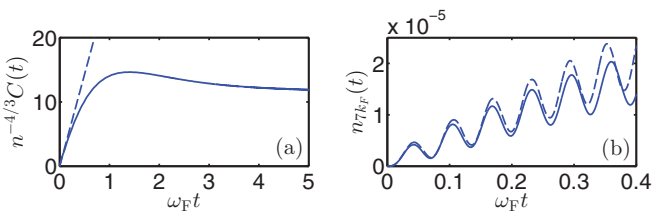

FIG. 3. (Color online) (a) Saturation of the contact as a function of time (blue solid line). The dashed line shows Eq. (5), valid at short times. (b) Comparison of two-body (dashed) and many-body (solid) momentum occupation at $k = 7k_F$ as a function of time.

[Eq. (2)]. However, comparing with the experimental data of Ref. [22], we find compelling validation that this approach captures the essential physics of the *large-momentum modes*. Indeed, by fitting our numerical data for the contact to an exponential function $\Delta C(1 - e^{-t/\tau_C})$ (exactly as in Ref. [22]), we find $\tau_C \approx 0.4/\omega_F \approx 23\ \mu$s, consistent with the measured equilibration time of the largest momenta modes (see Fig. 5 of Ref. [22]).

Three-body model. One of the crucial results of Ref. [22] is the long time scale for three-body loss relative to the observed dynamics at unitarity. With a goal of understanding this separation of time scales, we introduce a model which quantifies three-body loss when the energy scale is principally determined by the density rather than temperature or scattering length. To our knowledge, this is the first model of its kind.

To begin, we recall the known result that, for temperatures $k_B T \gg \hbar^2/(ma^2)$, three-body loss, described by the rate equation $\dot{n} = -L_3 n^3$, is independent of a [19,44]:

$$L_3(k_B T) = \frac{36\sqrt{3}\pi^2}{m^3}\frac{(1 - e^{-4\eta})}{(k_B T)^2}\hbar^5, \tag{6}$$

where $\eta > 0$ is the inelasticity parameter (whose value depends on atomic species), accounting for decay into deeply bound dimer states (see Sec. 7 of Ref. [15]). However, Eq. (6) fails when the gas temperature is below degeneracy: the energy scale $k_B T$ in Eq. (6) should approximate the average collision energy between three particles [44], but at zero temperature in a unitary Bose gas, this scale is set by the density (i.e., Fermi energy), *not* the temperature. Substituting $k_B T \to \hbar\omega_F$ in Eq. (6), for the ^{85}Rb experiment [22] ($n \approx 5.5 \times 10^{12}$ cm^{-3} and $\eta \approx 0.06$ [45]), we find a lifetime of about 0.20 ms. Although this estimate is in reasonable agreement with the observed value of $\tau_{exp} \approx 0.63$ ms, we stress that this approach is based purely on dimensional analysis and is derived from the concept of three-body scattering, which loses meaning for $na^3 \gg 1$.

In order to understand three-body loss under nonequilibrium conditions and account for density-dependent effects (naturally introducing the role of the Fermi energy), we numerically solve the three-body problem with $a = \infty$ [46,47] in an artificial harmonic trap [48,49] whose confinement length a_{ho} is fixed by the density of the many-body system, analogous with our two-body model (Fig. 1). Our observed agreement between two- and many-body models provides some additional motivation for proceeding as such. References [25,26] provide additional precedent for this. The inclusion of a third particle, however, introduces an entirely new set of states (Efimov states) which have no counterpart in the set of two-body eigenstates [15]. In our model, each three-body eigenstate has a finite width (denoted by Γ_β, where β is used to label the eigenstates). This width corresponds to a finite lifetime of the respective state due to decay into a deeply bound dimer plus a free atom and it is parametrized by the inelasticity parameter η (see [32] and Sec. 7.2 of Ref. [15]). Here, we adjust our model to reproduce the correct value for the width of the lowest Efimov state: $\Gamma_0 = 4\eta/s_0 E_0$ [15,32]. One important aspect of our approach is that it does not rely on the concept of scattering. For our nonequilibrium scenario,

we define the *effective* recombination rate as (see Ref. [32])

$$L_3^* = \frac{1}{n^2}\sum_\beta \left[|c_\beta(a_{\rm ho})|^2 \frac{\Gamma_\beta(a_{\rm ho})}{\hbar}\right]. \quad (7)$$

Here, c_β is the probability amplitude of populating the three-body state β after instantaneously switching a from $a \approx 150a_0$ (a_0 being the Bohr radius) to $a = \infty$. For the parameters of the experiment of Ref. [22], this leads to an average lifetime of $\tau_{\rm loss} = 1/(n^2 L_3^*) \approx 1.1$ ms, consistent with the observation. To test the robustness of this result, we allow variations of $a_{\rm ho}$ up to $\pm 50\%$ which leads to variations in the lifetime from 0.56–2.13 ms. Even the lower limit of this lifetime is considerably longer than our estimate for the equilibration time scale of large-momentum modes $\tau_{\rm C} = 0.4/\omega_{\rm F} \approx 23\ \mu$s, obtained from our many-body theory. We find that L_3^* depends on η as $L_3^* \propto \eta$ [consistent with Eq. (6)]. We thus suggest a universal formula $\tau_{\rm loss}/\tau_{\rm C} \approx \alpha/\eta$, where α is a dimensionless constant. Our model predicts $\alpha \approx 2.87$. This implies in the case of ^{85}Rb ($\eta \approx 0.06$) $\tau_{\rm loss}/\tau_{\rm C} \approx 47.8$; for ^{7}Li, $\eta \approx 0.21$ [19], and we find $\tau_{\rm loss}/\tau_{\rm C} \approx 13.7$; for ^{133}Cs, η ranges from 0.08–0.19 for different Feshbach resonances [50], implying $\tau_{\rm loss}/\tau_{\rm C} \approx 15.1$–$35.9$; and finally for ^{39}K, $\eta \approx 0.09$ [20], hence $\tau_{\rm loss}/\tau_{\rm C} \approx 31.9$.

The key ingredient of such long lifetimes is that the quench populates only long-lived three-body states whose sizes are comparable to the mean interparticle spacing (see Ref. [32]). In fact, we note that the population of the lowest Efimov state c_0^2 is negligible due to its relatively small size. That is crucial for the stability of the system at nonequilibrium since this state has the shortest lifetime (1 μs) due to a large weight at small hyperradius. Indeed, all states (including excited Efimov states) which do overlap considerably with the initial state typically have a small probability of finding all three particles within a small volume $\sim r_{\rm vdW}^3$, and therefore have much longer lifetimes. These conclusions do not hold for quenches that are adiabatic.

In summary, we have explored the short-time evolution of a degenerate Bose gas upon quenching to an infinite scattering length. We introduced and solved few- and many-body models to understand the evolution of the momentum distribution, with a particular focus on large-momentum modes. We found an oscillation period associated with each momentum mode and observed that it scales as $1/k^2$, demonstrating how dynamics of higher-momentum modes occurs more rapidly than lower-momentum modes. We found $1/k^5$ dependence in the momentum distribution due to nonequilibrium two-body correlations. We predicted a linear growth of Tan's contact at short times [see Eq. (5) and surrounding text], and observed a saturation time scale of $\tau_{\rm C} \approx 0.4/\omega_{\rm F}$. We introduced a model for calculating three-body loss at finite density and calculated the characteristic time scale of loss to be significantly longer than $\tau_{\rm C}$, robust to quite large changes in our model parameters. These findings are consistent with experimental results [22]. In closing, we remark that the final (quasi)equilibrium state of the system following such a quench is beyond the scope of our current theory. At longer times, effects due to correlations between larger numbers of particles presumably become important [36,51,52]. Understanding the nature of these higher-order correlations, and at which time scales they present themselves, remains for future work.

Acknowledgments. We acknowledge S. Natu, E. Mueller, C. Klauss, P. Makotyn, L. Radzihovsky, V. Gurarie, D. Jin, and E. Cornell for suggestions. We gratefully acknowledge funding from the NSF (J.L.B.), ARO MURI (A.G.S.), NDSEG fellowship program (J.P.C. and A.P.K.), AFOSR MURI and NSF (J.P.D. and C.H.G.), and NSF-PFC (K.R.A.H. and A.M.R.). K.R.A.H. thanks the NRC for support. This manuscript is the contribution of NIST, an agency of the US government, and is not subject to US copyright.

[1] C. Chin, R. Grimm, P. Julienne, and E. Tiesinga, Rev. Mod. Phys. **82**, 1225 (2010).
[2] D. S. Petrov, C. Salomon, and G. V. Shlyapnikov, Phys. Rev. Lett. **93**, 090404 (2004).
[3] J. Kinast, A. Turlapov, J. E. Thomas, Q. Chen, J. Stajic, and K. Levin, Science **307**, 1296 (2005).
[4] J. T. Stewart, J. P. Gaebler, C. A. Regal, and D. S. Jin, Phys. Rev. Lett. **97**, 220406 (2006).
[5] M. Horikoshi, S. Nakajima, M. Ueda, and T. Mukaiyama, Science **327**, 442 (2010).
[6] D. T. Son and E. G. Thompson, Phys. Rev. A **81**, 063634 (2010).
[7] S. Nascimbene, N. Navon, K. J. Jiang, F. Chevy, and C. Salomon, Nature (London) **463**, 1057 (2010).
[8] M. J. H. Ku, A. T. Sommer, L. W. Cheuk, and M. W. Zwierlein, Science **335**, 563 (2012).
[9] S. B. Papp *et al.*, Phys. Rev. Lett. **101**, 135301 (2008).
[10] N. Navon *et al.*, Phys. Rev. Lett. **107**, 135301 (2011).
[11] P. O. Fedichev, M. W. Reynolds, and G. V. Shlyapnikov, Phys. Rev. Lett. **77**, 2921 (1996).
[12] E. Nielsen and J. H. Macek, Phys. Rev. Lett. **83**, 1566 (1999).
[13] B. D. Esry, C. H. Greene, and J. P. Burke, Jr., Phys. Rev. Lett. **83**, 1751 (1999).
[14] P. F. Bedaque, E. Braaten, and H.-W. Hammer, Phys. Rev. Lett. **85**, 908 (2000).
[15] E. Braaten and H.-W. Hammer, Phys. Rep. **428**, 259 (2006).
[16] C. Langmack, D. H. Smith, and E. Braaten, Phys. Rev. Lett. **111**, 023003 (2013).
[17] N. R. Claussen, E. A. Donley, S. T. Thompson, and C. E. Wieman, Phys. Rev. Lett. **89**, 010401 (2002).
[18] T. Weber, J. Herbig, M. Mark, H.-C. Nägerl, and R. Grimm, Phys. Rev. Lett. **91**, 123201 (2003).
[19] B. S. Rem *et al.*, Phys. Rev. Lett. **110**, 163202 (2013).
[20] R. J. Fletcher, A. L. Gaunt, N. Navon, R. P. Smith, and Z. Hadzibabic, Phys. Rev. Lett. **111**, 125303 (2013).
[21] W. Li and T.-L. Ho, Phys. Rev. Lett. **108**, 195301 (2012).
[22] P. Makotyn, C. E. Klauss, D. L. Goldberger, E. A. Cornell, and D. S. Jin, Nature Physics (2014), doi:10.1038/nphys2850.
[23] With some similarities to a recent preprint, see X. Yin and L. Radzihovsky, Phys. Rev. A **88**, 063611 (2013).

[24] T. Busch, B.-G. Englert, K. Rzaźewski, and M. Wilkens, Found. Phys. **28**, 549 (1998).
[25] B. Borca, D. Blume, and C. H. Greene, New J. Phys. **5**, 111 (2003).
[26] K. Góral, T. Köhler, S. A. Gardiner, E. Tiesinga, and P. S. Julienne, J. Phys. B: At., Mol. Opt. Phys. **37**, 3457 (2004).
[27] S. Tan, Ann. Phys. (NY) **323**, 2952 (2008); **323**, 2971 (2008); **323**, 2987 (2008).
[28] E. Braaten and L. Platter, Phys. Rev. Lett. **100**, 205301 (2008).
[29] S. Zhang and A. J. Leggett, Phys. Rev. A **79**, 023601 (2009).
[30] P. Nozieres and D. Saint James, J. Phys. (Paris) **43**, 1133 (1982).
[31] J. L. Song and F. Zhou, Phys. Rev. Lett. **103**, 025302 (2009).
[32] See Supplemental Material at http://link.aps.org/supplemental/10.1103/PhysRevA.89.021601 for additional details of our calculations.
[33] G. E. Astrakharchik, J. Boronat, J. Casulleras, and S. Giorgini, Phys. Rev. Lett. **93**, 200404 (2004).
[34] E. Braaten, D. Kang, and L. Platter, Phys. Rev. Lett. **106**, 153005 (2011).
[35] Y. Castin and F. Werner, Phys. Rev. A **83**, 063614 (2011).
[36] D. Hudson Smith, E. Braaten, D. Kang, and L. Platter, arXiv:1309.6922.
[37] The Fermi momentum and energy simply give us convenient units when the interparticle spacing is the only length scale, no notion of fermionization (as in that which occurs in strongly interacting one-dimensional bosons) is implied by using such units.
[38] S. S. Natu and E. J. Mueller, Phys. Rev. A **87**, 053607 (2013).
[39] A. Rancon, C.-L. Hung, C. Chin, and K. Levin, Phys. Rev. A **88**, 031601(R) (2013).
[40] C.-L. Hung, V. Gurarie, and C. Chin, Science **341**, 1213 (2013).
[41] J. M. Diederix, T. C. F. van Heijst, and H. T. C. Stoof, Phys. Rev. A **84**, 033618 (2011).
[42] J. J. R. M. van Heugten and H. T. C. Stoof, arXiv:1302.1792.
[43] H. T. C. Stoof and J. J. R. M. van Heugten, J. Low Temp. Phys. **174**, 159 (2014).
[44] J. P. D'Incao, H. Suno, and B. D. Esry, Phys. Rev. Lett. **93**, 123201 (2004).
[45] R. J. Wild, P. Makotyn, J. M. Pino, E. A. Cornell, and D. S. Jin, Phys. Rev. Lett. **108**, 145305 (2012).
[46] H. Suno, B. D. Esry, Chris H. Greene, and James P. Burke, Jr., Phys. Rev. A **65**, 042725 (2002).
[47] J. Wang, J. P. D'Incao, B. D. Esry, and C. H. Greene, Phys. Rev. Lett. **108**, 263001 (2012).
[48] D. Blume and C. H. Greene, Phys. Rev. A **66**, 013601 (2002).
[49] F. Werner and Y. Castin, Phys. Rev. Lett. **97**, 150401 (2006).
[50] M. Berninger *et al.*, Phys. Rev. Lett. **107**, 120401 (2011).
[51] L. Platter, H.-W. Hammer, and Ulf-G. Meißner, Phys. Rev. A **70**, 052101 (2004).
[52] S. Piatecki and W. Krauth, arXiv:1307.4671.

Supplementary material for: Quenching to unitarity: Quantum dynamics in a 3D Bose gas

A. G. Sykes,[1] J. P. Corson,[1] J. P. D'Incao,[1] A. P. Koller,[1] C. H. Greene,[2] A. M. Rey,[1] K. R. A. Hazzard,[1] and J. L. Bohn[1]

[1] *JILA, University of Colorado and National Institute of Standards and Technology, Boulder, Colorado 80309-0440, USA*
[2] *Dept. of Physics, Purdue University, West Lafayette, Indiana 47907-2036, USA*

Many-body model: The equations of motion for the many-body model are given by

$$i\hbar\dot{c}_0 = nU(0)c_0 + \frac{1}{V}\sum_{\mathbf{k}\neq 0} U(\mathbf{k})\frac{c_0^* g_{\mathbf{k}} + c_0 \left|g_{\mathbf{k}}\right|^2}{1-\left|g_{\mathbf{k}}\right|^2} \quad (1)$$

and

$$\begin{aligned} i\hbar\dot{g}_{\mathbf{p}} =& 2\left(\epsilon_{\mathbf{p}} + nU(0)\right) g_{\mathbf{p}} + \frac{U(\mathbf{p})}{V}\left[c_0^2 + c_0^{*2} g_{\mathbf{p}}^2 + 2\left|c_0\right|^2 g_{\mathbf{p}}\right] \\ &+ \frac{1}{V}\sum_{\mathbf{k}\neq 0} U(\mathbf{p}-\mathbf{k})\frac{2\left|g_{\mathbf{k}}\right|^2 g_{\mathbf{p}} + g_{\mathbf{k}} + g_{\mathbf{k}}^* g_{\mathbf{p}}^2}{1-\left|g_{\mathbf{k}}\right|^2}, \end{aligned} \quad (2)$$

the numerical solutions of which are described in the main text.

Two-body model: We find an analytic formula for the Fourier transform of the eigenstates of two interacting atoms in a harmonic trap (following Reference [23] of the main text) at unitarity,

$$\begin{aligned} \tilde{\psi}_\nu(\mathbf{k}) =& \frac{4\pi A_\nu}{\tilde{k}}\left[(-2)^{\nu+3/2}\mathrm{Q}_{2\nu+1}(\tilde{k}) + \right. \\ & \left. \sqrt{2}(-1)^{\nu+1/2}\,\mathrm{F_D}\left(\frac{\tilde{k}}{\sqrt{2}}\right)\mathrm{H}_{2\nu+1}(\tilde{k})\right] \end{aligned} \quad (3)$$

where $\tilde{k} = k a_{\mathrm{ho}}$ is a dimensionless momentum, $\mathrm{F_D}$ is the Dawson integral, and

$$\begin{aligned} Q_m(k) =& m!\sum_{l=0}^{m/2}\frac{(-1)^{m/2-l}2^{2l}}{(2l)!(m/2-l)!}\times \\ & \sum_{n=\max(0,\lceil\frac{2l-m-1}{2}\rceil)}^{\lfloor l-1/2\rfloor}(2n-1)!!\,k^{2l-2n-1} \end{aligned} \quad (4)$$

is a polynomial ($\lfloor\cdot\rfloor$ and $\lceil\cdot\rceil$ indicate the floor and ceiling functions respectively).

To extract the behavior of the contact from our results, we find the asymptotic form of $\tilde{\psi}_\nu(\mathbf{k})$ as $k\to\infty$,

$$\tilde{\psi}_\nu(\mathbf{k}) \to a_{\mathrm{ho}}^{3/2}(-1)^{\nu+1/2}2^{1-\nu}\pi^{1/4}\sqrt{\frac{\Gamma(2+2\nu)}{\Gamma(3/2+\nu)}}\frac{1}{\tilde{k}^2}. \quad (5)$$

Using this formula, along with the expression for the overlap integral c_ν given in the main text, we find

$$n^{(2\mathrm{B})}_{k\to\infty} = \frac{4a_{\mathrm{ho}}^3}{\pi^{7/2}\tilde{k}^4}\left|\sin(\omega_{\mathrm{ho}}t)\right|, \quad (6)$$

and since we only trust the correspondence between the model and the physical system at times small compared to the harmonic oscillator time, we Taylor expand to get $n^{(2\mathrm{B})}_{k\to\infty} = \frac{4a_{\mathrm{ho}}^3}{\pi^{7/2}\tilde{k}^4}\omega_{\mathrm{ho}}t$.

Finally, we note that $n_k^{(2\mathrm{B})}$ is normalized such that $\int d^3\mathbf{k}\, n_k^{(2\mathrm{B})} = 1$, as opposed to the usual many-body normalization where n_k is dimensionless and $\int \frac{d^3\mathbf{k}}{(2\pi)^3}\, n_k = n$. Multiplying Eq. (6) by $(2\pi)^3 n$, and using the relationship between a_{ho} and n proposed in the main text, yields Eq. (5) of the main text.

Large-momentum, short time two-body dynamics: As described in the main text, the key features of the dynamics of the two-body model are captured by a simple, analytic formula [Eq. (4), main text] that is valid for momenta large compared to the inverse of the length scale of the confining potential. Due to the agreement of the two-body and many-body-variational descriptions at short times and large momentum, this formula describes the many-body-variational results as well.

Equation (4) in the main text captures the characteristic fast oscillations at momentum k with timescale $\tau_k = \mu/(\hbar k^2)$, and the linear rise in the $1/k^4$ tail. As argued in the main text, up to a constant prefactor the dynamics in this large-momentum, short-time limit result should be independent of the details of the effective trapping potential used. We have explicitly verified this by comparing calculations for a spherical box with hard walls, the harmonic oscillator model introduced in the main text, and a continuum model described below.

We briefly sketch the derivation. We work in a continuum, and will regularize all wavefunctions by assuming a decay $e^{-r/(2L)}$, with L large compared to other scales in the problem; such regularization is implicit in the equations below. We assume the system starts in a non-interacting wavefunction with momentum k_0 in relative spherical coordinates

$$\phi_{k_0}(r) = A_{k_0}\sin(k_0 r)/r \quad (7)$$

where the normalization A_{k_0} matters only for the prefactor. The eigenstates for atoms interacting with a pseudopotential at unitarity are

$$\varphi_p(r) = B_p\cos(pr)/r \quad (8)$$

where B_p is a normalization factor. The eigenenergies are $\hbar^2k^2/(2\mu)$. The time dependence of the two-body

wavefunction is then given by

$$\phi_{k_0}(r,t) = \int_0^\infty dp\, c_{k_0 p}\varphi_p(r) e^{-i\hbar^2 k^2 t/(2\mu)}, \qquad (9)$$

where $c_{k_0 p}$ is the projection of ϕ_{k_0} on φ_p. Calculating these coefficients and the integral over p, and from this calculating the momentum distribution $n_k = (2\pi)^3 n |\int d^3r\, e^{i\vec{k}\cdot\vec{r}}\phi_{k_0}(r,t)|^2$, we find the formula given by Eq. (4) in the main text.

Three-body model: For our numerical calculations, the *effective* recombination rate [see Eq. (7) of the main text] was calculated from the solutions of the three-body problem in hyperspherical coordinates [1, 2]. Here, the total three-body wave function can be written as

$$\Psi(R,\Omega,t) = \sum_\beta c_\beta \Psi_\beta(R,\Omega)\exp[-iE_\beta t/\hbar], \qquad (10)$$

where R is the hyperradius and Ω is the set of hyperangles [1]. In the above equation, E_β and Ψ_β are the energies and eigenstates of the post-quench Hamiltonian whose artificial harmonic trap width ($a_{\rm ho}$) is set by the density of the many-body system, and $|c_\beta|^2$ is the population the final states after the quench, given by;

$$c_\beta = \int dR\, d\Omega\, J(R,\Omega)\Psi(R,\Omega,t=0)\Psi_\beta(R,\Omega), \qquad (11)$$

where J is the Jacobian of the transformation from cartesian to hyperspherical coordinates. The initial condition, $\Psi(R,\Omega,t=0)$, is chosen to be the lowest three-body trap state for small values of a ($\sim 150a_0$). Our numerical calculations were performed using the Lennard-Jones potential model for the two-body interactions adjusted in order to produce the desired scattering length [2].

We introduce a decay/loss mechanism to the three-body states in the trap by artificially coupling each eigenstate to a deeply bound dimer-atom channel (see section 7 of Ref. [3]). The binding energy of the dimer (typically on the order of 1eV$\sim 10^4$K) is sufficiently large that the kinetic energy of the free atom would greatly exceed any realistic trapping potential, and all three atoms are lost from the trap. We have tested this artificial-channel-coupling model against more realistic numerical calculations (where deeply bound states were actually present) and obtained excellent agreement. The net result of this procedure is to obtain three-body energy levels in the trap which possess a finite width, given by Γ_β, and we should replace Eq. (10) by

$$\Psi(R,\Omega,t) = \sum_\beta c_\beta \Psi_\beta(R,\Omega)\exp[-i(E_\beta - i\Gamma_\beta/2)t/\hbar]. \qquad (12)$$

In our numerical calculations we adjust the width of the lowest Efimov state such that $\Gamma_0 = 4\eta/s_0 E_0$ [3], where η is the species dependent inelasticity parameter, $s_0 \approx 1.00624$, $E_0 = \hbar^2\kappa_*^2/m \approx 0.051\hbar^2/m r_{\rm vdW}^2$ and $r_{\rm vdW}$ is the van der Waals length [2]. Experimental measurements tell us: $\eta = 0.06$ for ^{85}Rb [4], $\eta = 0.21$ for ^{7}Li [5], η=0.08-0.19 for ^{133}Cs [6], and $\eta = 0.09$ for ^{39}K [7]. Our model incorporates the recently discovered universality of the three-body parameter κ_* (see Ref. [2] and references therein).

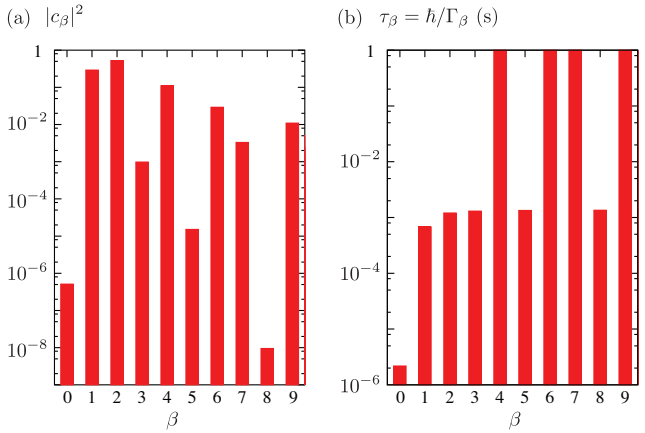

FIG. 1: (Color online) (a) Population, c_β, and (b) lifetimes, $\tau_\beta = \hbar/\Gamma_\beta$, of three-body states after the quench. The vanishingly small population of the lowest Efimov state, c_0^2, whose lifetime is about 1μs, ensures the longer experimental lifetimes, provided by the population of excited states.

For a given value of $a_{\rm ho}$, we can now obtain a lifetime due to three-body decay implied from the finite width of the states. The time evolution of atomic density at short times can be written in terms of the normalization (which is no longer conserved) of the wavefunction at time t, $\int dR d\Omega J(R,\Omega)|\Psi(R,\Omega,t)|^2$, as

$$\begin{aligned} n(t) &= n(0)\int dR\, d\Omega\, J(R,\Omega)|\Psi(R,\Omega,t)|^2 \\ &= n(0)\sum_\beta |c_\beta(a_{\rm ho})|^2 \exp[-\Gamma_\beta(a_{\rm ho})t/\hbar]. \end{aligned} \qquad (13)$$

Finally, the effective recombination rate is defined by $L_3^* = -\lim_{t\to 0}\dot{n}(t)/n^3(t)$, and setting $n(0) = n$ yields Eq. (7) of the main text:

$$L_3^* = \frac{1}{n^2}\sum_\beta \left[|c_\beta(a_{\rm ho})|^2 \frac{\Gamma_\beta(a_{\rm ho})}{\hbar}\right]. \qquad (14)$$

Figure 1 shows some of the results from our numerical calculations illustrating the populated levels, c_β^2, and the corresponding lifetimes, $\tau_\beta = \hbar\Gamma_\beta$, for the value of $a_{\rm ho}$ adjusted to reproduce the value of the average density of the ^{85}Rb experiment ($n \approx 5.5\times 10^{12}$cm^{-3}). As one can see, the population of the lowest Efimov state, c_0^2, is negligible. This is due to the fact that the size of that state, $\kappa_*^{-1} \approx 4.4 r_{\rm vdW}$ [2], is much smaller than the average interatomic distance, $n^{-1/3}$. According to our calculations, and evidently from Eq. (11), all the states

with substantial population are of sizes comparable to the size of the initial state before the quench, i.e., they have sizes comparable to the mean interatomic distance, and lifetimes much longer than the lowest Efimov state [see Fig. 1 (b)].

[1] H. Suno, B. D. Esry, Chris H. Greene, and James P. Burke, Jr., Phys. Rev. A **65**, 042725 (2002).

[2] J. Wang, J. P. D'Incao, B. D. Esry, and C. H. Greene, Phys. Rev. Lett. **108**, 263001 (2012).

[3] E. Braaten and H.-W. Hammer, Phys. Rep. **428**, 259 (2006).

[4] J. R. Wild, P. Makotyn, J. M. Pino, E. A. Cornell, and D. S. Jin, Phys. Rev. Lett. **108**, 145305 (2012).

[5] B. S. Rem, *et al.*, Phys. Rev. Lett. **110**, 163202 (2013).

[6] M. Berninger, *et. al.*, Phys. Rev. Lett. **107**, 120401 (2011).

[7] R. J. Fletcher, A. L. Gaunt, N. Navon, R. P. Smith, and Z. Hadzibabic, Phys. Rev. Lett. **111**, 125303 (2013).